



Hardware-in-the-Loop Evaluation of an Advanced Distributed Energy Resource Management Algorithm

Preprint

Jing Wang, Jeff Simpson, Rui Yang, Bryan Palmintier, Soumya Tiwari, and Yingchen Zhang

National Renewable Energy Laboratory

*Presented at the 2021 IEEE Innovative Smart Grid Technologies, North America (ISGT NA)
February 16–18, 2021*

**NREL is a national laboratory of the U.S. Department of Energy
Office of Energy Efficiency & Renewable Energy
Operated by the Alliance for Sustainable Energy, LLC**

This report is available at no cost from the National Renewable Energy Laboratory (NREL) at www.nrel.gov/publications.

Contract No. DE-AC36-08GO28308

Conference Paper
NREL/CP-5D00-80765
September 2021



Hardware-in-the-Loop Evaluation of an Advanced Distributed Energy Resource Management Algorithm

Preprint

Jing Wang, Jeff Simpson, Rui Yang, Bryan Palmintier, Soumya Tiwari, and Yingchen Zhang

National Renewable Energy Laboratory

Suggested Citation

Wang, Jing, Jeff Simpson, Rui Yang, Bryan Palmintier, Soumya Tiwari, and Yingchen Zhang. 2021. *Hardware-in-the-Loop Evaluation of an Advanced Distributed Energy Resource Management Algorithm: Preprint*. Golden, CO: National Renewable Energy Laboratory. NREL/CP-5D00-80765. <https://www.nrel.gov/docs/fy21osti/80765.pdf>.

© 2021 IEEE. Personal use of this material is permitted. Permission from IEEE must be obtained for all other uses, in any current or future media, including reprinting/republishing this material for advertising or promotional purposes, creating new collective works, for resale or redistribution to servers or lists, or reuse of any copyrighted component of this work in other works.

**NREL is a national laboratory of the U.S. Department of Energy
Office of Energy Efficiency & Renewable Energy
Operated by the Alliance for Sustainable Energy, LLC**

This report is available at no cost from the National Renewable Energy Laboratory (NREL) at www.nrel.gov/publications.

Contract No. DE-AC36-08GO28308

Conference Paper
NREL/CP-5D00-80765
September 2021

National Renewable Energy Laboratory
15013 Denver West Parkway
Golden, CO 80401
303-275-3000 • www.nrel.gov

NOTICE

This work was authored in part by the National Renewable Energy Laboratory, operated by Alliance for Sustainable Energy, LLC, for the U.S. Department of Energy (DOE) under Contract No. DE-AC36-08GO28308. Funding provided by the U.S Department of Energy Office of Energy Efficiency and Renewable Energy Solar Energy Technologies Office Enabling Extreme Real-Time Grid Integration of Solar Energy (ENERGISE) program Agreement Number 32960. The views expressed herein do not necessarily represent the views of the DOE or the U.S. Government.

This report is available at no cost from the National Renewable Energy Laboratory (NREL) at www.nrel.gov/publications.

U.S. Department of Energy (DOE) reports produced after 1991 and a growing number of pre-1991 documents are available free via www.OSTI.gov.

Cover Photos by Dennis Schroeder: (clockwise, left to right) NREL 51934, NREL 45897, NREL 42160, NREL 45891, NREL 48097, NREL 46526.

NREL prints on paper that contains recycled content.

Hardware-in-the-Loop Evaluation of an Advanced Distributed Energy Resource Management Algorithm

Jing Wang, Jeff Simpson, Rui Yang, Bryan Palmintier, Soumya Tiwari, Yingchen Zhang
Power Systems Engineering Center, National Renewable Energy Laboratory Golden, CO 80401, USA
Jing.Wang@nrel.gov, Yingchen.Zhang@nrel.gov

Abstract—This paper presents the laboratory performance evaluation of voltage regulation under a new distributed energy resource management system (DERMS) algorithm via an advanced hardware-in-the-loop (HIL) platform. The HIL platform provides realistic testing in a laboratory environment, including the accurate modeling of a full-scale real-world distribution system from a utility partner, the DERMS software controller, and power hardware photovoltaic (PV) inverters. The new DERMS algorithm is developed based on online multi-objective optimization (OMOO) algorithms that perform fast dispatch of distributed solar PV simulated in a real-time digital simulator and real physical hardware devices. Experimental tests confirm the correct functioning of the HIL platform for evaluating controller algorithms and satisfactory voltage regulation performance of the developed OMOO algorithms.

Index Terms—distributed energy resource management system (DERMS), hardware-in-the-loop (HIL), online multi-objective optimization (OMOO), voltage regulation.

I. INTRODUCTION

With the rapid integration of distributed energy resources (DERs) in distribution systems, more utilities face challenges integrating large numbers of non-utility devices into operations at all levels [1]. Industry and IEEE working groups have begun to address DER integration by identifying, standardizing, and requiring the functions that individual DERs can perform autonomously, such as frequency-watt and voltage-volt ampere reactive (Volt-var) controls [2]. However, in many situations, significantly improved performance can be achieved with centralized coordination of distribution assets using advanced distribution management systems (ADMS) or other feeder-wide coordination systems such as distributed energy resource management systems (DERMS) [3].

ADMS is a software platform that integrates numerous utility systems [1], including supervisory control and data acquisition (SCADA), geographic information system, outage management system, etc., and provides a suite of different functionalities such as voltage optimization. DERMS have been

This work was supported by Alliance for Sustainable Energy, LLC, the manager and operator of the National Renewable Energy Laboratory for the U.S. Department of Energy (DOE) under Contract No. DE-AC36-08GO28308. This material is based upon work supported by the U.S. Department of Energy's Office of Energy Efficiency and Renewable Energy (EERE) under Solar Energy Technologies Office (SETO) Agreement Number 32962. The views expressed in the article do not necessarily represent the views of the DOE or the U.S. Government. The U.S. Government retains and the publisher, by accepting the article for publication, acknowledges that the U.S. Government retains a nonexclusive, paid-up, irrevocable, worldwide license to publish or reproduce the published form of this work, or allow others to do so, for U.S. Government purposes.

an emerging technology that bridges the gap between DER group-managing entities (e.g., ADMS) and DER devices to aggregate, monitor, and control groups of DERs as a simpler, more manageable set of services [4]. DERMS projects are diverse in scale, objectives, and types of DERs, but the goals are similar: provide grid services (e.g., voltage regulation, peak load management, and respond to interruptions and outages), improve controllability and observability of DERs, enable interoperability of DERs and coordination with legacy devices, and explore the potential for customer engagement in supporting the grid. To move the ADMS and DERMS technology forward, research and evaluations are needed to ensure that the DERMS work as expected before field deployment. Therefore, a generic test bed for evaluating coordinated control among ADMS, other utility management systems (e.g., DERMS), DERs, and legacy utility equipment controllers (e.g., capacitor banks and voltage regulator controllers) was developed in [5] to provide a realistic laboratory testing environment, including real-time co-simulation of full-scale distribution systems provided by utility partners, controller and power hardware, and industry standard communications protocols.

This work builds on this testbed and showcases its ability to simulate an advanced control algorithm's interaction with a simulated utility power system with a high penetration of solar photovoltaics (PV) and to evaluate the resulting voltage regulation performance. The software controller dynamically interacts with not only a distribution feeder model, but also a sub-transmission model via with real-time measurements, dispatched power setpoints, and hardware inverters through standard communications protocols as if the controller were interacting with real-world systems in the field. In addition, this advanced HIL platform can efficiently evaluate the control solution in a variety of system configurations and operational scenarios, which helps utility partners understand the technical benefits of deploying any controllers for large-scale DER integration and management. The setup in this project showcases the testbed's flexibility to focus on specific control function to coordinate distribution resources for system level target functions to also support early stage validation.

II. OVERVIEW OF THE HIL SETUP

This HIL platform validates the optimization and control solution against a simulated real-world distribution system, using data provided by the Hawaiian Electric Company, with over 2,000 nodes. A co-simulation platform is used to simulate the sub-transmission system in OpenDSS and the whole distribution feeder in a digital real-time simulator, OPAL-RT. The DERMS algorithm is implemented in Python and integrated into the co-simulation platform through the Hierarchical Engine

for Large-scale Infrastructure Co-Simulation (HELICS) [6]. An overview of the HIL setup is shown in Fig. 1. The main elements of the test bed are the co-simulation (OpenDSS, HELICS, and OPAL-RT), software controller HIL (grid optimization), and power HIL (five physical PV inverters). Each main element is explained in detail below.

A. Co-simulation Platform

Simulating the large number of nodes in an electromagnetic transient (EMT) real-time simulation, such as OPAL-RT's eMegaSim, is problematic because of computational challenges. Simulating a subtree in EMT and the rest of the system in a quasi-steady-state power flow solver, such as OpenDSS is also an option; but was not selected due to possible numerical instability caused by the closed loop of the PHIL interactions. Instead, we opted to simulate the whole distribution feeder in a phasor-domain, real-time simulation using ePhasorSim from OPAL-RT. The sub-transmission is simulated with quasi-steady-state time-series simulation in OpenDSS, as shown in Fig. 1. Both sub-transmission and distribution feeder can be modelled in OPAL-RT. Since there is no PHIL to be tested with sub-transmission, we simulate it in OpenDSS.

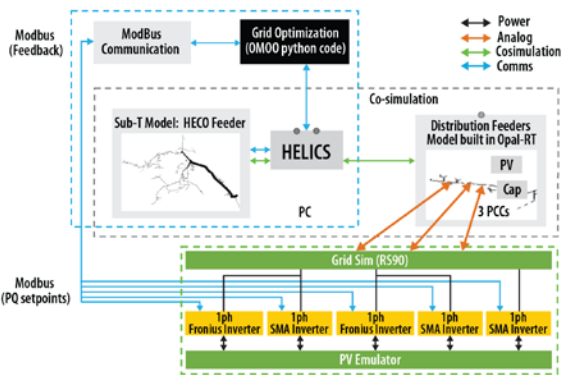


Figure 1. Overall diagram of the integrated HIL platform.

The ePhasorSim model in OPAL-RT is converted from OpenDSS using a conversion tool. Fig. 2 shows the validation results from this conversion. The ePhasorSim and OpenDSS voltages match very well across the feeder. We computed an average error of -0.001198%, standard error of 0.002617%, and maximum error of 0.01416%.

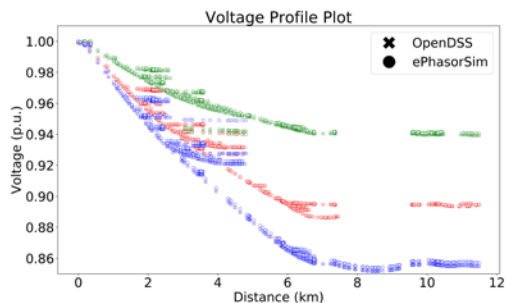


Figure 2. Validation of the OpenDSS and ePhasorSim models.

In ePhasorSim the feeder has a peak load of 3 MW and approximately 1,827 three-phase nodes. There are 245 customers, and each customer has distributed PV installed sized to meet half of the peak load capacity. The simulation includes capacitor bank, at the end of the feeder, working in autonomous control. Load and PV production data are based on utility

SCADA system measurements in a resolution of 4-8 seconds. One representative day is selected, and the data is interpolated to a 1-minute resolution. In OpenDSS, the sub-transmission system has 176 nodes, 10 customers, and no PV.

HELICS is used to synchronize the two simulation platforms and enable the communications for data exchange. The voltage magnitude and phase angle at the distribution feeder head node in OPAL-RT are provided by the OpenDSS simulation of sub-transmission, and the measured active and reactive power of the feeder head in OPAL-RT are sent back to OpenDSS to close the simulation loop [7]. In addition, the load profiles for the 10 loads in OpenDSS are sent from OPAL-RT to ensure that all loads read the load profiles at the same time stamp.

B. Grid Optimization for DER Management

The Grid Optimization algorithm under test, the online multi-objective optimization (OMOO) scheme, was developed as an extension of the algorithm from [8]. A high-level representation of OMOO flow and implementation for dispatching distributed DERs is shown in Fig. 3. As described in [8], the OMOO is implemented in a centralized manner which consists of local controllers and a central controller. Each local controller implements setpoints issued by the central controller and communicates the objective function and constraints on the feasible setpoints to the central controller. In turn, the central controllers use these information and its system-wide voltage measurements to compute the next feasible setpoints for the local controllers. This algorithm is computationally affordable for solving the optimal power flow of a large-scale system, and it can perform online convex optimization to provide fast updates for power set points in real time (seconds level).

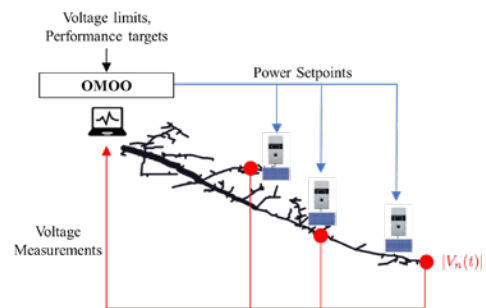


Figure 3. OMOO flow for dispatching distributed DERs.

C. DER Assets and Power Hardware-in-the-Loop

Power-hardware-in-the-loop (PHIL) is used to integrate actual PV inverter power hardware with the controller. Specifically, OMOO provides optimal power set points to hardware inverters and the testbed enables measuring the actual response. As shown in Fig. 1, there are five PV inverters under test, installed at three DER racks. Each rack represents a point of common coupling (PCC) connected at a simulated node in the OPAL-RT model. Rack 1 and Rack 2 both have one 3-kVA SMA PV inverter and one 5-kVA Fronius PV inverter, and Rack 3 has only one 3-kVA SMA PV inverter. A PV emulator with multiple modules is used to power the DC side of the PV inverters, and each module follows a V-I curve to emulate the operation of maximum power point tracking of a solar panel. All the PV inverters are configured to work in PQ dispatch mode and communicate with the external controller via a ModBus communications protocol.

Each DER rack is interfaced with the distribution feeder simulated in OPAL-RT through a grid simulator (AC power supply) independent phase control allowing support for all the three single-phase PCCs—Phase A for PCC 1, Phase B for PCC 2, and Phase C for PCC 3. The simulated voltage in OPAL-RT is scaled down and sent out through analog outputs to the grid simulator. This scaled voltage is then reconstructed by the grid simulator to a physical voltage (240 V) and fed to the hardware PV inverters. At each PCC, the inverter outputs the desired amount of active and reactive power, and the lumped voltage and current are measured by a potential transformer and current transformer, respectively, and then sent back to OPAL-RT through analog inputs. In OPAL-RT, the voltage and current are then scaled up to replicate the actual measured voltage and current at the PCC. In the end, the calculated active and reactive powers are scaled up to the simulated capacity and feed the controlled current source to close the PHIL loop. Note that some calibration measures described in [9] are carried out in OPAL-RT to ensure that the calculated active and reactive power match the measured power at each PCC before scaling up to the simulated capacity. The OMOO dispatches the power references to the hardware inverters and receives the feedback power measurements of the current source replicating the hardware inverters in the OPAL-RT, which forms the closed-loop testing of the control system and makes the OMOO controller act as if it interacts with all real hardware in the field.

D. ModBus Communication

In this HIL setup, the computer embedded with the grid optimization algorithm needs to control the hardware PV inverters by sending real and reactive power setpoints. A ModBus communications agent is implemented in the HELICS platform to work as an interface between the grid optimization controller and the hardware inverters. The computer is defined as the ModBus master, and the five hardware PV inverters are ModBus slaves. The active and reactive power reference for each inverter are passed from the grid optimization control to the ModBus agent. Then the ModBus agent calls the ModBus interface functions, reaches each hardware inverter through the IP address of the inverter, writes the registers for the active and reactive power references, and reads the registers for the active and reactive power measurements.

III. IMPLEMENTATION OF THE INTEGRATED HIL PLATFORM

HELICS is the key player in this integrated platform to merge all the elements (software and hardware), synchronize them, allocate the execution time of each element and transfer data between elements. Fig. 4 shows a high-level structure of HELICS and the data exchange between elements. Four agents are included in the HELICS framework: the OPAL agent, OpenDSS agent, OMOO agent, and ModBus agent. The HELICS agents inherit data from a base agent class to abstract the publish and subscription aspects of HELICS. The agents also get base setup information from a file that provides the location for the distribution feeder model inputs and the agent results outputs and defines the time/update frequency-related information. The execution time step for each agent is 0.1 s for the OPAL agent, 4 s for the OpenDSS agent, 10 s for the OMOO, and 10 s for the ModBus agent. Note that we define the ModBus agent run period as every 10 s to allow all PV inverters settle to a steady state before the next reference comes in.

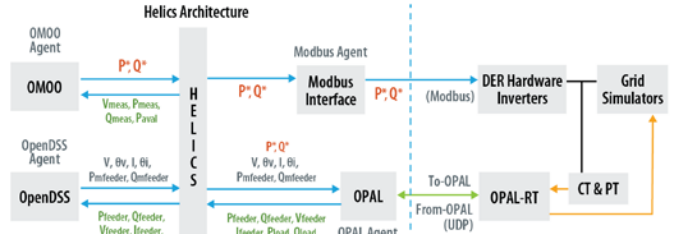


Figure 4. Schematic diagram of the HELICS architecture.

All agents are value federates, and the values are transferred as strings. The keys for each value transfer between two agents are enumerated in a mapping file. If a key-value pair is missing, it can be caught by comparing against what is expected. As shown in Fig. 4, there are five value transfer paths: OpenDSS to OPAL, OPAL to OpenDSS, OMOO to OPAL, OPAL to OMOO, and OMOO to ModBus. The OPAL agent is a data aggregator between the real-time simulator OPAL-RT and the two agents (OpenDSS and OMOO); thus, all the data to OPAL-RT and from OPAL-RT are also defined in the dictionary. The data from OPAL-RT (From-OPAL) are received by the OPAL agent and then extracted for the OpenDSS agent and OMOO agent to run in real time. Similarly, all the data sent to OPAL-RT (To-OPAL) are packed together and then sent to OPAL-RT through the OPAL agent. Note that the communications between the HELICS computer and the OPAL-RT is set up through UDP protocol with predefined port number and IP address, and the OPAL agent calls the UDP socket function for communications and defines the data encoding and decoding for data transfer.

Fig. 5 shows the flowchart of the operation of each agent in the HELICS framework. The time values in the left part of the figure show the execution time of each agent, and the right part shows the time offset from the execution time of each agent to perform the data exchange (publish and subscribe). The OpenDSS agent is the time flag. It runs every 4 s (defined by Time_freq) and performs the data exchange with a time offset of $\Delta t1$ (0 ms, means no offset). The other agents follow a similar operation. For example, the OMOO agent runs every $T2$, and it performs the data exchange with a time offset of $\Delta t4$. This allows each agent federate to run at the fixed time step and synchronize the data transfer and system dynamics in real time. More implementation details of HELICS can be found in [9].

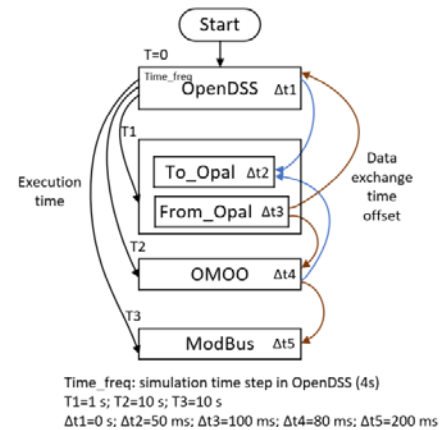


Figure 5. Flowchart of HELICS configuration.

After setting up the HELICS framework and integrating the OMOO control code, the HELICS computer is configured to have two local area networks so that it can communicate with both the OPAL-RT and hardware inverters.

For the PHIL implementation, the simulated DER capacities for the three PCCs are 23.5 kVA, 19.5 kVA, and 93.9 kVA, which are larger than the actual capacities for the hardware inverters connected at each PCC; thus, the active and reactive power references for each PCC is scaled down according to the total capacity of the connected hardware inverter(s) and shared proportionally among inverters at each PCC. At the OPAL-RT side, the active and reactive power are filtered with a low-pass filter and then scaled up to the simulated capacity.

Because there are hardware inverters to be tested, special caution needs to be taken in terms of start-up and shutdown of the inverters and hardware setup to avoid any harmful transients or undesired responses from the inverters (i.e., a timeout error). During the startup process, empirical initial power references (close to the dispatched values when HELICS starts to run) are given to the hardware inverters. This allows the inverters to generate smooth power when HELICS is enabled and keeps the inverters “awake.” Otherwise, the inverter(s) might go into standby mode, not respond the control command, and cause a timeout error in the ModBus agent. This will fail the test. For the shutdown procedure, zero active and reactive power references are given to the hardware inverters to avoid opening the switch at high current and power.

Once all the elements are integrated and working, a communications test is performed to ensure that data are transferred correctly and timely between agents. Finally, the actual experiment is carried out to evaluate the voltage regulation performance against the target voltage and to ensure that the distribution model is stable. In the end, the operation procedures are developed to have all elements run smoothly: turn on the hardware inverters, give initial power references to the hardware inverters, start the simulation in OPAL-RT, start HELICS, enable the PV controls if power references are received in OPAL, close the PHIL switch, enable data saving, and start reading the load and PV profiles.

IV. EXPERIMENTAL RESULTS

This section presents the HIL experimental results that demonstrate the voltage regulation performance of the developed grid optimization algorithm, OMOO. Of particular interest is how the OMOO dispatches the actual hardware inverters, the real response of the inverters, and the interactions between the OMOO controller and the hardware inverters. For the evaluation, the 2-h simulation window from 10:00 a.m.–12:00 p.m. is selected to capture voltage issues that might result from high injections from PV with low loads. The load and PV profiles are presented in Fig. 6, which shows that the power generated by PV is higher than the active power demand. In this test, 242 PVs are simulated in OPAL-RT and 3 PVs are represented by the actual power measured from the DER racks as shown in Fig. 1. All those PVs are controlled by the software controller OMOO.

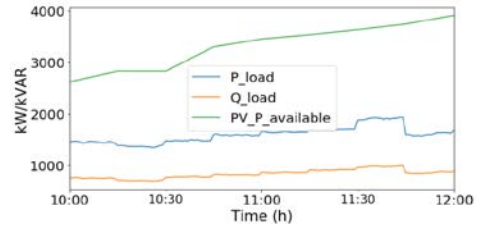


Figure 6. Load and PV profiles used for the HIL evaluation.

The baseline mode without any DERMS control (PV working in unity power factor mode) is simulated, and the voltage measurements are presented in Fig. 7 (a). The difference between the maximum and minimum voltages is less than 0.02 p.u. across the whole feeder with 1,827 nodes, which indicates that the selected utility feeder is a stiff feeder. Therefore, the upper and lower limits for the voltage set points in the OMOO are cautiously selected as 0.95 p.u. and 1.03 p.u., and the acceptable error is 0.002 p.u. Significant effort was made to tune the global gradient descent step and the local gradient descent step in each PV local controller and to set the objective penalty for active power curtailment. The tuned results are shown in Fig. 7 (b), which shows maximum voltage regulated around the target value, 1.03 p.u., and a calculated maximum error of 0.0016 p.u. The voltage regulation performance is acceptable with the stiff grid.

The results of the total PV measurements are shown in Fig. 8. In the baseline, the PV_{total} matches the available PV. However, since the PV inverter is not oversized, the total PV active power under OMOO control is curtailed slightly to allow reactive power absorption to regulate the voltage within the operating limits. The calculated total curtailment is 4.23% of the total solar energy (MWh) in the baseline scenario.

To further show the voltage regulation performance, one control parameter output, tot_muk, related to the upper voltage violation of the OMOO is presented in Fig. 9. Tot_muk becomes zero when the system voltages are less than the upper limit, and it changes to nonzero to drive the PV local controllers to reduce active power generation and increase reactive power contribution for collective voltage regulation. The higher the overvoltage violation, the larger this value becomes. Once all the voltages are regulated gradually, tot_muk starts to decrease, and it becomes zero again when there are no high-voltage violations. The response of tot_muk shows that the OMOO converges and responds correctly to the system dynamics to output the control parameters for voltage regulation.

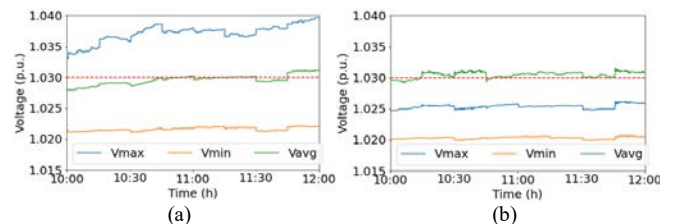


Figure 7. Voltage measurements of the distribution feeder: (a) baseline mode without control and (b) with OMOO control evaluated in the HIL.

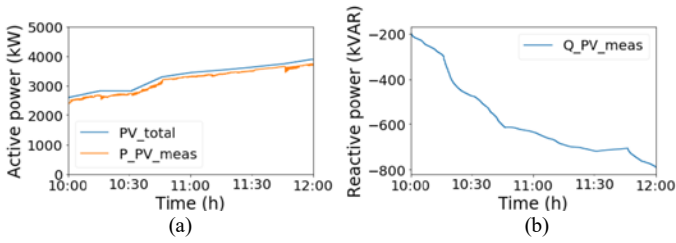


Figure 8. Measurements of total PV: (a) available active power and measured active power output and (b) measured reactive power output.

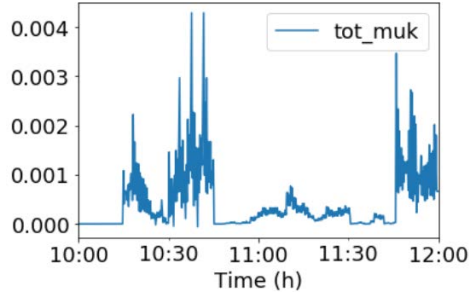


Figure 9. Control parameter, tot_muk which relates to overvoltage violation.

Fig. 10 presents the experimental results of the PHIL testing of three PCCs with five PV hardware inverters to demonstrate the real dynamics and responses of the hardware interacting with the OMOO controller. The results show the active and reactive power reference from the OMOO (orange line) and the closed-loop PHIL active and reactive power injection (blue line) for each PCC, respectively. All the plots show that the closed-loop PHIL injection follows the dispatched power reference. Note that the reactive power reference is small for the first PCC, and satisfactory tracking performance is still achieved thanks to the compensation and calibration work, particularly for the reactive power. The dynamics of the active power reference for each PCC look similar, and the same is true for reactive power, even though each PCC has unique dynamics in measured active and reactive power from the actual hardware inverters. The dynamics (ripples) in the measured hardware inverter output power will be replicated and reflected in the current controlled source in OPAL-RT and influence the dynamics of the PCC voltage.

Below, we explore one simulated PV in the OPAL-RT with the highest PCC voltage to investigate the dynamics of active and reactive power with high terminal voltages. The results show that there is noticeable active power curtailment (1.55%), and the reactive power contribution is large—in fact, the largest in all 245 PV inverters. The curtailment level is lower than the total curtailment level (4.23%). Because the PV curtailment level depends on the terminal voltage, also the sensitivity matrix. The curtailment level is not that high. It can mean that it will not impact much the voltage by reducing active power.

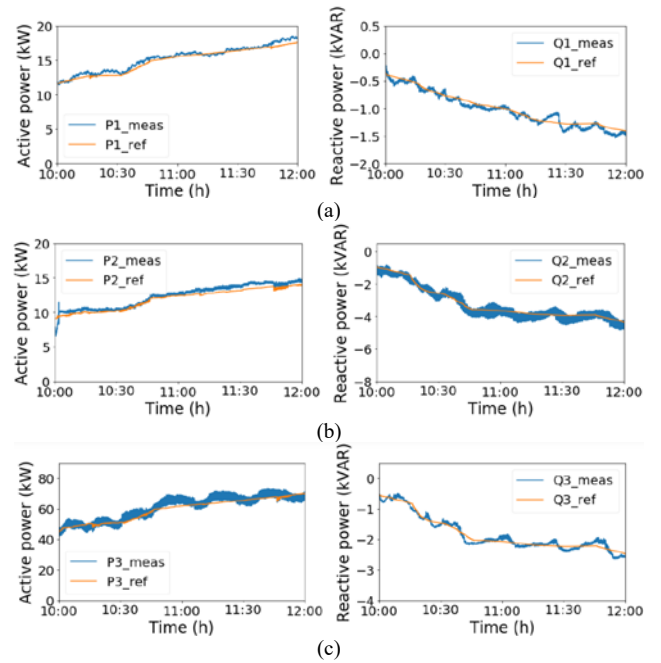


Figure 10. Experimental results of the three PCCs (active power (left) and reactive power (right)): (a)(b)(c) power reference and PHIL closed-loop injection at PCC 1, 2 and 3 respectively.

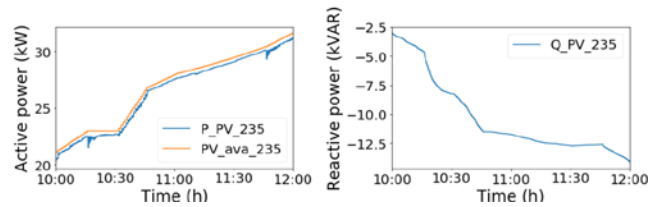


Figure 11. Measurements of simulated PV with highest PCC voltage.

The PCC voltages of the three PHILs (Fig. 10) and the simulated PV (Fig. 11) are presented in Fig. 12 to show the relationship between the reactive power and the PCC voltage. Even though there are ripples in the inverters' power outputs, the PCCs with hardware inverter(s) are still stable. The voltage at PCC 1, V1, is the lowest among the four voltages, and the reactive power contribution is smallest. Similarly, the voltage at the simulated PV, V615, is the highest, and the reactive power is largest. The results indicate that higher voltage results in larger reactive power contribution for voltage regulation (if the capacity is permitted), which is consistent with the control design of the OMOO that the reactive power contribution mainly depends on the terminal voltage (the network sensitivity is another factor).

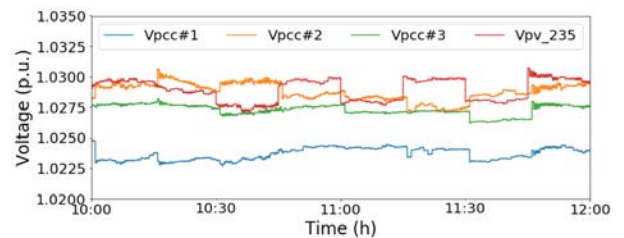


Figure 12. PCC voltages of the three PHILs and simulated PV 235.

The results presented in this section demonstrate two important aspects: 1) the developed HIL platform is effective to evaluate DER management for voltage regulation with real-time modeling of the distribution feeder, controller software in the loop, and PHIL testing of physical inverter hardware; and 2) the OMOO algorithm is effective at voltage regulation.

V. CONCLUSIONS

This paper presents the performance evaluation of a DERMS control algorithm using an advanced HIL platform. The HIL platform includes co-simulation of the distribution feeder, the software controller of the distribution grid optimization, and the power hardware PV inverters. HELICS is the key tool to integrate all the software and hardware and allows the software controller to interact with the real-time simulation model and hardware inverters as if the controller were interacting with a real-world system. The detailed implementation of such an integrated platform is described to give readers a useful reference for establishing such a platform. The high-fidelity, real-time test of a high-voltage scenario with realistic load and PV profiles demonstrates the effectiveness of the voltage regulation algorithm and captures the system-level impacts and operation of the distribution feeder with both the CHIL and PHIL. The results also show the value of using this advanced HIL platform to evaluate the DER management system based on real-world distribution systems.

ACKNOWLEDGMENTS

The authors thank Marc Asano and his team from Hawaiian Electric providing the data, and NREL colleagues for the following support: Blake Lundstrom and Peter Gotseff for their help using the DER racks, Michael Blonsky for supporting the HELICS development, Wenbo Wang and Dheepak Krishnamurthy for converting the model from OpenDSS to ePhasorSim, and Andrey Bernstein for supporting the algorithm development.

REFERENCES

- [1] Jan Vrins, Global Energy Practice Lead, Distributed Energy Resource, <https://www.navigant.com//media/www/site/downloads/energy/2016/distributedenergyresourcesimpactsonstrategybusiness.pdf>.
- [2] B. Seal, A. Renjit, and B. Deaver, 2018, Understanding DERMS, CA: Electric Power Research Institute, <https://www.epri.com/#/pages/product/000000003002013049/?lang=en>.
- [3] K. A. W. Horowitz, et al., "A Techno-economic Comparison of Traditional Upgrades, Volt-Var Controls, and Coordinated Distributed Energy Resource Management Systems for Integration of Distributed Photovoltaic Resources," *Electrical Power and Energy Systems*, 123 (2020) 106222, May 2020.
- [4] Microgrid Knowledge: What are Distributed Energy Management Systems (aka DERMS)? Available: <https://microgridknowledge.com/derms-next-generation-grid/>.
- [5] A. Pratt, M. Baggu, F. Ding, S. Veda, I. Mendoza, E. Lightner, "A Test Bed to Evaluate Advanced Distribution

Management Systems for Modern Power Systems," *IEEE Eurocon 2019*, Novi Sad, Serbia, July 1-4, 2019.

- [6] B. Palmintier, et al., "Design of the HELICS high-performance transmission-distribution-communication-market co-simulation framework," *Workshop on Modeling and Simulation of Cyber-Physical Energy Systems (MSCPES)*, Pittsburgh, PA, 2017, pp. 1-6.
- [7] J. Wang, et al., "Performance Evaluation of Distributed Energy Resource Management via Advanced Hardware-in-the-Loop Simulation," *IEEE Conference on Innovative Smart Grid Technologies (ISGT)*, Washington, DC, USA, Feb. 17-20, 2020.
- [8] A. Bernstein and E. Dall'Anese, "Bi-level dynamic optimization with feedback," *2017 IEEE Global Conference on Signal and Information Processing (GlobalSIP)*, Montreal, QC, 2017, pp. 553-557.
- [9] GMLC-TDC/HELICS: Hierarchical Engine for Large Scale Infrastructure Co-Simulation. Available: <https://github.com/GMLC-TDC/HELICS>.